Combustion Science and Technology, 1981, Vol. 26, pp. 193–201
0010-2202/81/2606-0193$06.50/0

The Effect of Room Openings on Fire Plume Entrainment

J. G. QUINTIERE, W. J. RINKINEN and W. W. JONES *National Bureau of Standards*

(*Received March 11, 1981; in final form May 11, 1981*)

Abstract—The mass rate of entrainment is examined for a fire plume in a room. Entrainment rates are inferred from measurements of air flow through a door or window and from room temperature data. The effect of the air flow is to tilt the flame plume, and to increase the entrainment rate over that of a vertical free standing plume. Dimensional analysis and theoretical results for a non-reacting wind blown plume model are used to correlate the flame angle and entrainment rate results. *Key words;* entrainment, flame angle, room fire, openings, plume.

1 INTRODUCTION

The modeling of fires in enclosures requires an understanding and prediction of the air entrainment by the fire and the flow rate through room openings. Recent studies of fire plumes and their entrainment by McCaffrey (1979) and Zukoski, Kubota and Cetegen (1980) have shown that buoyant diffusion flames tend to entrain more than an idealized point source plume, and that the entrainment rate is influenced by burner diameter and laboratory atmospheric disturbances. Furthermore McCaffrey and Rockett (1977), in an analysis of small and large scale room fire experiments, show that their calculated entrainment rates are higher than the results predicted by the flame plume model of Steward (1970). These results implied required entrainment coefficients as high as 0.4 (compared to conventional values of about 0.1) to achieve agreement between the measured values and predicted results of Steward's model. These differences suggest that a better model is needed to predict entrainment or that the present models may not be applicable for a fire in a room. Because entrainment results have been established only for plumes downstream of their heat source, entrainment near the base region might not be accurately predicted from a one-dimensional integral model. On the other hand, disturbances due to room effects could invalidate the use of a free plume model in room fires. Recent experimental results have demonstrated an effect on a fire plume centered in the room, by the incoming flow through a room opening. This interaction influenced the flame orientation and the entrainment rate. These results will be presented and discussed.

2 EXPERIMENTAL DESIGN

Experiments were conducted in a room-fire-induced-flow facility which is explained more fully in a report by Steckler (1980). Figure 1 displays the overall arrangement of measurement probes and room geometry. Fourteen experiments were conducted in which the fire size was varied (62.9, 158 kW), and the room opening configuration was varied as shown in Figure 2 to form a door or a window. These openings were centered on one wall and aligned with the burner as shown for the door opening in Figure 1. The room dimensions were 2.8 m × 2.8 m × 2.13 m high with a 30 cm diameter porous plate diffusion flame burner centered and flush mounted with the floor. The fuel was methane and was supplied at a fixed rate of flow. A vertical array of aspirated thermocouples measured the room temperatures near a corner, and a vertical array of probes in the centerline of the room opening determined the temperatures and velocities. These data were recorded over a ten minute test duration in three second intervals. A television camera recorded the flame orientation from a side window. A grid pattern was electronically superimposed in the vertical plane of the flame image in order to determine the flame angle. The flame angle was determined over time by analyzing the video recording frame by frame. An average angle was defined over a radial distance

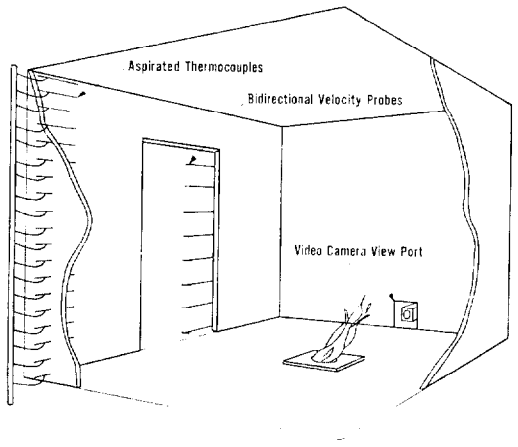

FIGURE 1 Experimental arrangement.

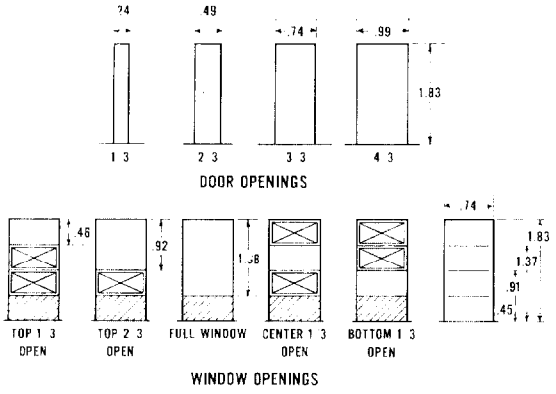

FIGURE 2 Door and window configurations and dimensions in *m*.

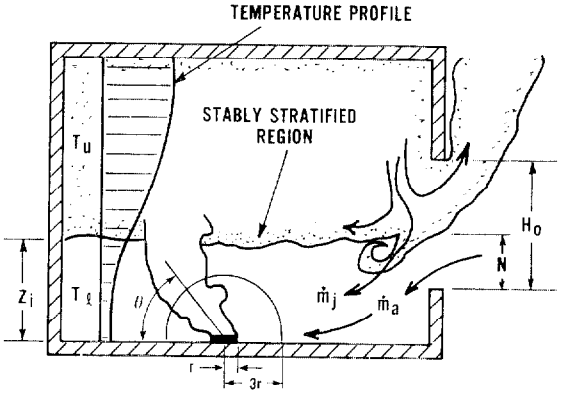

FIGURE 3 Flow dynamics.

equal to three times the burner radius. The sketch of the flame in Figure 3 gives a good illustration of the process of defining an angle.

3 EXPERIMENTAL RESULTS

Except for an initial transient response after the burner was ignited, the thermal and flow characteristics of the room gases were reasonably steady. A typical response is illustrated in Figure 4. There, it is seen that the flame is initially vertical and then moves to an inclined position in about 30 seconds by which time the flow pattern in Figure 3 is established. A representative upper room gas temperature response is also shown. It is seen that over most of the 10 minute test duration that nearly steady state conditions prevailed. The data to be presented and analyzed in this study apply to the

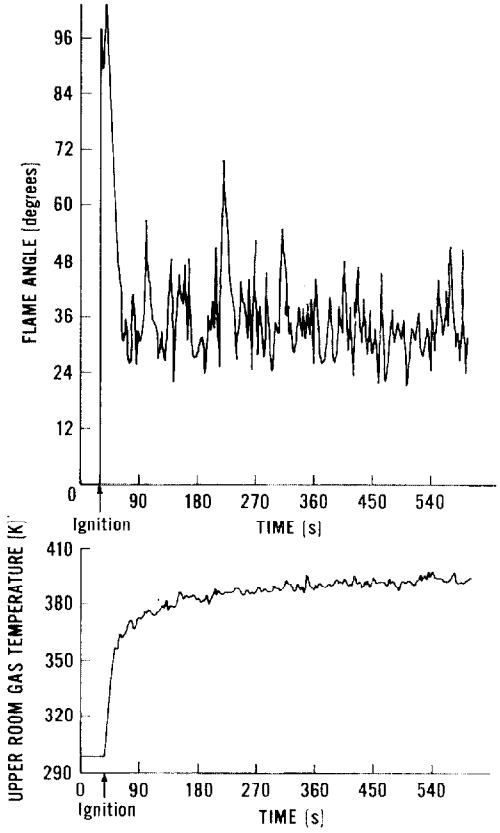

FIGURE 4 Typical flame angle and upper room gas temperature following ignition.

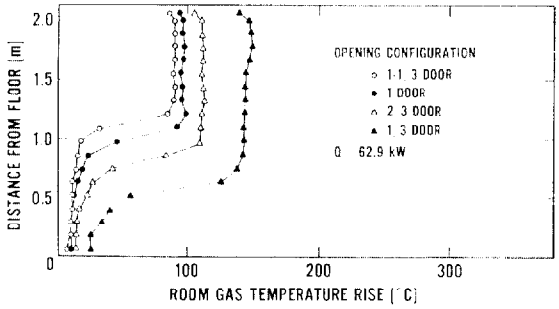

FIGURE 5a Room temperatures for door openings and $Q = 62.9$ kW.

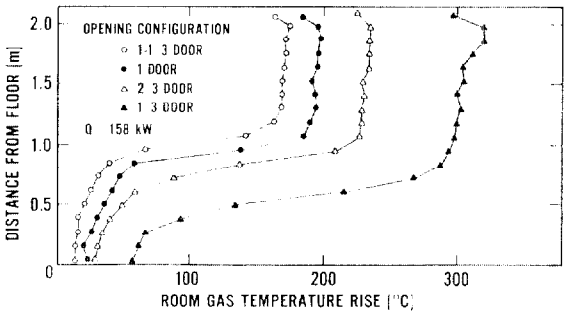

FIGURE 5b Room temperatures for door openings and $Q = 158$ kW.

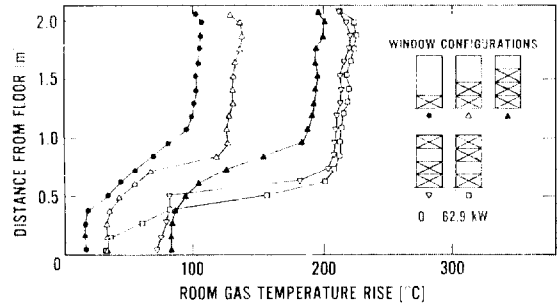

FIGURE 5c Room temperatures for window openings and $Q = 62.9$ kW.

"steady" conditions of the test. In particular, the flame angle is given as the time-averaged value with limits indicating its variation after the initial transient. The flame angle does fluctuate but not with a regular period. The "steady" gas temperatures were based on values measured at the end of the ten minute period.

To evaluate the *in-situ* entrainment characteristics of this fire plume, the rate of mass entrained ($\dot{m}_e$) and the vertical entrainment height need to be determined. Specifically for the application of modeling room fire flows, the rate of entrainment considered is taken from the fire base to the stably stratified gas region in the room. This is sketched in Figure 3. The effective entrainment height was determined from the thermal interface height (z_i) deduced from the vertical temperature profile in the room. This height was determined by the position of rapid temperature change between the lower and upper portions of the room. Due to diffusion and mixing this is not always a sharp designation; consequently, an entrainment height z_i could only be determined to within a ± 10 to ± 30 percent accuracy. The temperature profile results are shown in Figures 5a, b, and c.

The rate of fluid entrainment by the fire plume over the vertical distance z_i cannot be directly determined. As illustrated by the flow dynamics in Figure 3, fluid enters the lower layer (defined from the floor to z_i) as air flow through the opening ($\dot{m}_a$) and from the upper hot layer due to mixing near the opening ($\dot{m}_j$). For steady state conditions in a lower layer control volume that excludes the fire plumes and since no mixing occurs at height z_i (except for mass transport near the opening and at the plume), then the rate of entrainment over height z_i is given as

$$\dot{m}_e = \dot{m}_a + \dot{m}_j \tag{1}$$

The air flow rate, $\dot{m}_a$, has been obtained with good accuracy (within 10 percent) by velocity measurements (Steckler, 1980). However only an upper bound estimate can be given for $\dot{m}_j$ using the available data. It can be found by a balance on the lower layer which neglects heat transfer between the floor and the gas. Since the floor will be hotter than the gas due to radiation, the energy balance yields the upper limit of

$$(\dot{m}_j)_{\max} = \left(\frac{T_l - T_\infty}{T_u - T_l}\right) \dot{m}_a \tag{2}$$

where T_u is the mean upper layer gas temperature, T_l is the mean lower layer gas temperature, and T_∞ is the ambient air temperature. Hence upper and lower bounds can be determined for $\dot{m}_e$ as follows:

$$\dot{m}_a \leq \dot{m}_e \leq \dot{m}_a + (\dot{m}_j)_{\max} \tag{3}$$

TABLE I
Summary of results

Opening configuration	Opening width and height dimensions $W_0 \times H_0$ (m × m)	Fire size Q (kW)	Entrainment height z_i (m)	Flame angle θ (degrees)	Air mass flow rate $\dot{m}_a$ (kg/s)	Maximum mixing rate ($\dot{m}_j$) (kg/s)
4/3 Door	0.98 × 1.83	62.9	1.11±0.1	44±5	0.664	0.10
1 Door	0.74 × 1.83	62.9	0.97±0.1	38±5	0.561	0.087
2/3 Door	0.49 × 1.83	62.9	0.80±0.1	40±15	0.450	0.075
1/3 Door	0.24 × 1.83	62.9	0.51±0.1	37±5	0.261	0.062
4/3 Door	0.98 × 1.83	158	0.99±0.15	41±10	0.932*	0.116
1 Door	0.74 × 1.83	158	0.99±0.15	30±4	0.714	0.103
2/3 Door	0.49 × 1.83	158	0.80±0.15	55±5	0.533*	0.085
1/3 Door	0.24 × 1.83	158	0.57±0.2	55±5	0.257*	0.089
Full window	0.74 × 1.38	62.9	0.74±0.25	22±4	0.494	0.152
Top 2/3 window	0.74 × 0.92	62.9	0.68±0.20	27±4	0.293	0.102
Top 1/3 window	0.74 × 0.46	62.9	0.80±0.15	91±6	0.125	0.090
Center 1/3 window	0.74 × 0.46	62.9	0.57±0.05	85±10	0.099*	0.060
Bottom 1/3 window	0.74 × 0.46	62.9	0.46±0.1	56±5	0.099*	0.019
Full window	0.74 × 1.35	158	0.63±0.25	22±4	0.648*	0.097

*Indicates estimated value from temperature data

A complete summary of these results is given in Table I. In computing $(\dot{m}_j)_{\max}$ the mean upper and lower layer temperatures were selected from the temperature profile data as shown in Figure 5. The determination of $\dot{m}_a$ was taken from the results of Steckler (1980) for the cases in which these flame angle experiments were duplicates of his experiments. (The equivalence was substantiated by agreement in the temperature data between the two corresponding experiments). For the runs which were not duplicates, the rate of air flow was estimated from the temperature data by the equation (McCaffrey, 1970)

$$\dot{m}_a = 2.48\, W_0 \left[\frac{T_\infty}{T_u}\left(1-\frac{T_\infty}{T_u}\right)\right]^{1/2} (H_0 - N)^{3/2} \quad \text{(kg/s)} \quad (4)$$

where W_0 is the width of the opening in m, H_0 is the height of the opening in m, and N is the height of the neutral plane in the opening in m. The neutral plane height was determined from the velocity and temperature measurements in the opening. For the cases in which measured flow rates were available, the estimated results from Eq. (4) was within 10 percent of the measured value.

The rates of entrainment are plotted as a function of vertical distance (z_i) for the case of doorway openings in Figures 6a and window openings in Figure 6b. The experimental uncertainty in z_i is shown as well as the upper bound on the entrainment rate. The data points are plotted for the mean in the range of z_i and the lower bound for $\dot{m}_e = \dot{m}_a$. The range of z_i was determined by the region of minimum slope in the height versus temperature curves as shown in Figure 5. The theoretical prediction based on a free point source plume as taken from Zukoski *et al.* (1980) is also plotted. This result is

$$\dot{m}_{\text{pt}} = 0.210 \left(\frac{\rho_\infty{}^2 g}{c_p\, T_\infty}\right)^{1/3} Q^{1/3}\, z^{5/3} \quad (5)$$

where z is the vertical distance and Q is the heat source or corresponding rate of energy release by the fire.

It has been shown that, depending on the burner radius and flame height, Eq. (5) agrees with experimental values for undisturbed fire plumes within approximately ±30 percent (Zukoski *et al.*, 1980). Zukoski (1980) also found that disturbances due to adjoining walls or atmospheric turbulence have been found to result in entrainment rates as

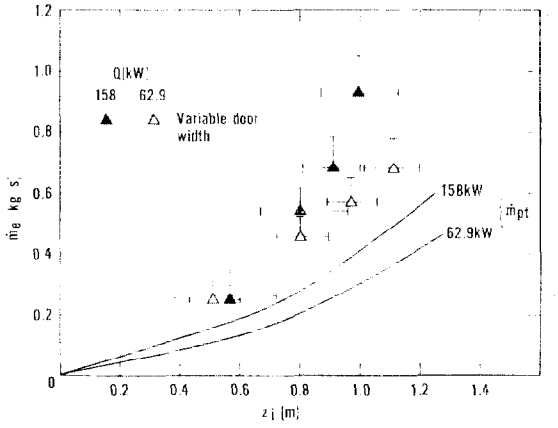

FIGURE 6a Fire plume entrainment with door openings.

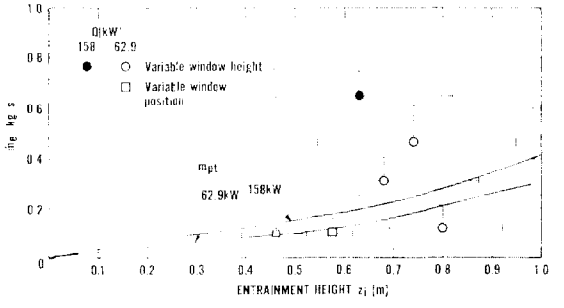

FIGURE 6b Fire plume entrainment with window openings.

high as 50 percent above $\dot{m}_{pt}$ from Eq. (5), and the measured results by McCaffrey (1979) yield results as high as 50 percent above $\dot{m}_{pt}$. However, as seen in Figures 6a and b, the results inferred from the room fires are generally well above the values anticipated for a free burning plume. On further examination of these results it was noted that fire plumes in the room which remained nearly vertical were in good agreement with $\dot{m}_{pt}$, *e.g.*, the top and center 1/3 windows. Plumes in which the opening "wind" effect led to a large flame tilt (small θ) had a much higher rate of entrainment than predicted by $\dot{m}_{pt}$, *e.g.*, the full window at 158 kW.

4 THEORETICAL CONSIDERATIONS

The theory of wind blown plumes was examined in order to arrive at a correlation and explanation of these results. The work of Hoult, Fay, and Forney (1969) was used as a basis for analysis.

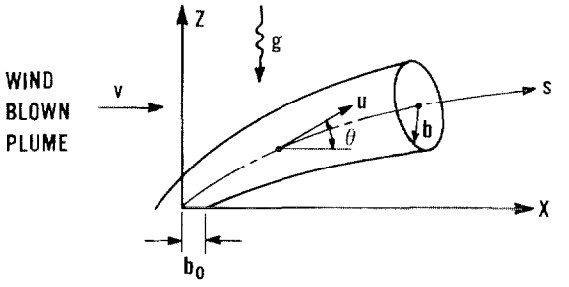

FIGURE 7 Wind blown plume variables.

That theory was developed to model wind blown effluent from a smoke stack, and was later extended to a turbulent diffusion flame in a cross flow by Escudier (1972) and Brzustowski (1978). These flame analyses were solved for the case of gas jets. Consequently their numerical results are not applicable to the case of low initial fuel velocity as in our experiments and other common natural fire plumes.

The theoretical model is based on an integral approach that considers entrainment to occur as a function of the plume velocity relative to its surroundings. A coordinate system and relevant variables are shown in Figure 7. The horizontal wind speed is given as v and the average (top-hat) plume velocity is given as u. The local entrainment velocity is assumed to be

$$v_{ent} = \alpha|u - v\cos\theta| + \beta|u\sin\theta| \qquad (6)$$

where α is the no-wind entrainment constant and β is an additional entrainment parameter due to the presence of a cross wind. Its value does not seem as universal as that of α. For example, Hoult (1969) finds $\beta = 0.6$ for laboratory data on smoke stacks and a best fit value of 0.9 for field data. Brzustowski (1972) used a value of $\beta = 0.13$ for a jet of propane burning in air.

Since a simple Boussinesq plume model is reasonably successful in predicting the entrainment rate of a free burning turbulent flame, its counterpart was considered for the cross wind case. The governing equations are found in Hoult *et al.* (1969) and in dimensionless variables are given below:

Mass

$$\frac{d}{d\xi}(UB^2) = 2B\,[\alpha|U - V\cos\theta| + \beta|V\sin\theta|] \qquad (7)$$

Momentum

$$\pi \frac{d}{d\xi}(B^2U^2) = \frac{\sin\theta}{U} + \pi V \cos\theta \frac{d}{d\xi}(B^2U) \tag{8}$$

$$\pi (B^2U^2)\frac{d\theta}{d\xi} = \frac{\cos\theta}{U} - \pi V \sin\theta \frac{d}{d\xi}(B^2U) \tag{9}$$

Energy

$$UB^2\phi = \frac{1}{\pi}\frac{{u_*}^2}{b_0 g} \tag{10}$$

The dimensionless variables are as follows:

$$\begin{aligned} &\text{plume radius, } B = b/b_0 \\ &\text{plume velocity, } U = u/u_* \\ &\text{wind velocity, } V = v/u_* \\ &\text{plume temperature, } \phi = (T - T_\infty)/T_\infty \\ &\text{position along the trajectory, } \xi = s/b_0 \end{aligned} \tag{11}$$

The normalizing parameters are given as follows:

T_∞ = ambient temperature
b_0 = plume initial radius

$$u_* = \left(\frac{Qg}{b_0 \rho_\infty T_\infty c_p}\right)^{1/3}, \text{ characteristic plume velocity}$$

From this formulation, it follows that the local trajectory angle depends on ξ and V. This implies that the average flame angle is only dependent on V; however, flames would follow a trajectory in a cross wind, and there would be no unique flame angle.

The other result of interest is the rate of entrainment. The cross wind model yields an entrainment rate which can be expressed as

$$\dot{m}_e = \pi \rho_\infty b_0^2 u_* [(UB^2)_{\xi=\xi_i} - (UB^2)_{\xi=0}] \tag{12}$$

where ξ_i is the trajectory position at the entrainment height corresponding to the layer position z_i. The ratio of this result with the point source free plume entrainment rate given in Eq. (5), suggests the following functional dependence:

$$\frac{\dot{m}_e}{\dot{m}_{pt}} = f(V, b_0/z_i) \tag{13}$$

These equations suggest the dimensionless variables that could be used to correlate the entrainment results for the room fire plume. Also their solution, with an initial condition corresponding to the experimental values, could provide useful quantitative results. Obviously, these results can only be considered semi-quantitative in view of the empirical parameter β in the model, the model's simplicity, and the complexity of the experimental conditions.

5 DIMENSIONAL ANALYSIS AND CORRELATIONS

It is expected that V is the primary dimensionless variable for correlating the measured flame angle θ and the entrainment ratio $\dot{m}_e/\dot{m}_{pt}$. A similar variable was used by Thomas *et al.* in correlating temperatures downwind of a line fire (1964) and for the height and length of wind blown crib flames (1963). Recently Raj *et al.* (1979) have correlated flame angles of wind blown LGN pool fires, and their result in terms of V is given as

$$\sin\theta = \begin{cases} 1 & , V' < 1 \\ \dfrac{1}{(V')^{1/2}} & , V' > 1 \end{cases} \tag{14}$$

in which $V' = V \Big/ \left(\dfrac{2c_p T_\infty \rho_\infty}{\pi \rho_f \Delta H}\right)^{1/3} = 5.26\, V$

for methane.

It was stated that Eq. (14) correlated their results to within 68 percent. Although other correlations exist for predicting flame angles (Pipkin *et al.*, 1964; Welker *et al.*, 1965) Eq. (14) is simplest to apply. It is used as a reference point for selecting a characteristic wind speed for the room fires.

The air flow induced by the room fire through the opening behaves as a jet; and for a window opening, it behaves more as an inverted plume. This jet or window plume entrains fluid within the room, some of it coming from the hot upper region of the room. The jet expands laterally as it flows toward the fire but can also contract in the vertical direction. The vertical height is the layer interface or entrainment height given as z_i. The width of the jet is initially the opening width, W_0, and can not exceed the room width W. Estimates based on a 2-D planar jet suggest a lateral increase from W_0 of 0.7 ± 0.2 m over the distance from the opening to the fire in the present case the average jet velocity just upwind of the fire would be the characteristic wind speed. This can be calculated as

$$v = \frac{\dot{m}_e}{\rho_j A_j} \tag{15}$$

where ρ_j and A_j are the jet density and cross-sectional area, respectively. Several choices were made in selecting the values of these quantities necessary to compute v. As stated, the flame angle results given in Eq. (14) were used as a reference for assessing the best choice of v. Also it was not appropriate to use an elaborate analysis due to the many uncertainties involved. Initially computing v as $\dot{m}_a/(\rho_\infty W z_i)$ yielded a good correlation for both θ and $\dot{m}_e/\dot{m}_{pt}$, but corresponding values of v given by Eq. (14) were approximately ten times higher. Consequently v was computed as

$$v = \frac{\dot{m}_a}{\rho_\infty W_0 z_i} \tag{16}$$

which when plotted against θ, as shown in Figure 8, appears to give results within the confidence limits asserted for Eq. (14). While this characteristic wind velocity appears to be appropriate for correlating these data, a more general analysis of the opening jet might be performed to obtain v for plumes at an arbitrary location in a room.

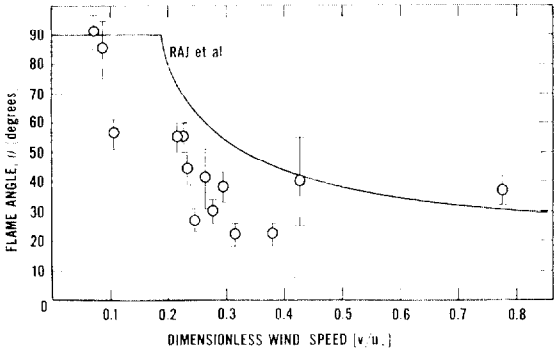

FIGURE 8 Flame angle as a function of v/u_*.

The dimensionless entrainment ratio is plotted with v/u_* in Figure 9. Although the value of (b_0/z_i) was considered, there is no noticeable trend that can be attributed to it. The outlying data above $v/u_* = 0.3$ scatter widely and the highest data point was based on an estimated, not measured value for $\dot{m}_a$. Below $v/u_* = 0.3$, the relationship between $\dot{m}_e/\dot{m}_{pt}$ and v/u_* is more discernible. In fact additional data from Steckler (1980) (not shown) would support the trend that $\dot{m}_e/\dot{m}_{pt}$ increases with the dimensionless wind speed. However, it should be realized that the wind speed

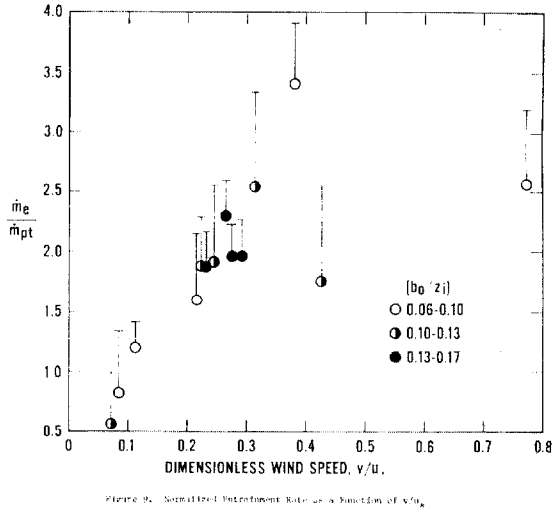

FIGURE 9 Normalized entrainment rate as a function of v/u_*.

and entrainment rate are coupled and not independent quantities. In fact, the variables plotted are defined as

$$\frac{\dot{m}_e}{\dot{m}_{pt}} = \frac{\dot{m}_a}{0.21\ \rho_\infty z_i^2 (b_0/z_i)^{1/3} u^*} \tag{17a}$$

and

$$\frac{v}{u_*} = \frac{\dot{m}_a}{\rho_\infty W_0 z_i u_*} \tag{17b}$$

which displays the coupling, and also the dependence on z_i which is a quality not precisely measured.

An alternative correlation for $\dot{m}_e/\dot{m}_{pt}$ is its dependence on flame angle. Since both of these variables depend on v/u_*, the uncertainty in defining v is eliminated by plotting them against each other. This is shown in Figure 10. A clear dependence of $\dot{m}_e/\dot{m}_{pt}$ with θ is displayed. Moreover, the data scatter about a $(\dot{m}_a/\dot{m}_{pt})$ equal to one, if $\dot{m}_{pt}$ is evaluated based on the inclined plume length, $z_i/\sin\theta$. This suggests a simple calculation for estimating $\dot{m}_e$ provided θ is known, but its general accuracy and validity are uncertain.

6 THEORETICAL RESULTS

A numerical solution to the wind blown plume equations was computed. A value of a was selected to insure that $\dot{m}_e/\dot{m}_{pt} = 1$ "far" from the source

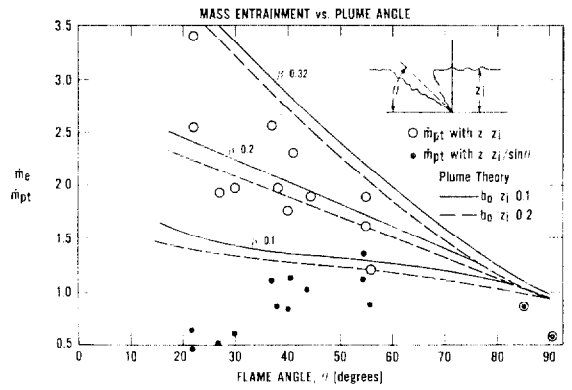

FIGURE 10 Normalized entrainment rate as a function of flame angle.

for $v = 0$. This was found to be 0.16 and is in agreement with the entrainment constant generally used for buoyant plumes. Various values for the second entrainment coefficient β were examined. A value of $\beta = 0.2$ was found to fit the data best. This is shown in Figure 10. Also shown is the variation in the theoretical results due to changes in b_0/z_i and β. The theoretical results with $\beta = 0.2$ are in good qualitative, but not necessarily good quantitative, agreement with the results for entrainment ratio and flame angle plotted against v/u_*. This suggests that the "wind" speed defined from the experimental data is not an accurate quantitative measure of the true effect of inflow on the fire.

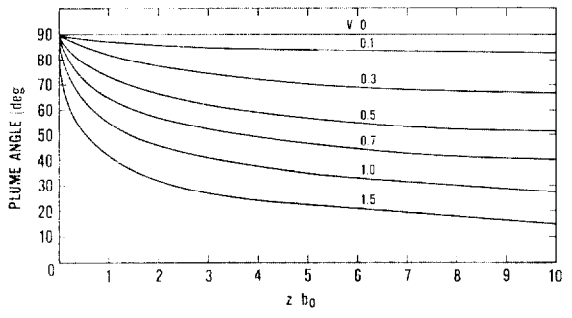

FIGURE 11 Theoretical local non-reacting plume angle for $\alpha = 0.16$ and $\beta = 0.2$.

The angle predicted from the plume model depends on trajectory position. Its variation is shown as a function of dimensionless height in Figure 11. The local plume angle for a given value of b_0/z_i was used in plotting the theoretical results in Figure 10. Although the theoretical predictions show a gradual change in angle for z/b_0 greater than 3, there is still some question of relating average experimental flame angle with the variable non-reacting plume prediction.

7 CONCLUSIONS

Fire plumes near a room opening have been shown to be affected by the air flow induced through the opening. This flow is coupled to the strength of the fire plume and the size and location of the opening. The phenomenon is similar to a fire plume in a cross wind. The theory of wind blown applies to this room fire problem to the extent that an equivalent wind speed can be identified for the room opening flow. This equivalence cannot be done perfectly and that is reflected in the results. However, a comparison between measured and theoretical results for normalized entrainment rate as a function flame angle eliminates the need to define the wind speed. In these variables, the experimental and theoretical results are in fair agreement when the second entrainment constant $\beta = 0.2$. These results have implications on the anticipated level of accuracy required in room fire modeling.

Room fire growth models (Emmons, 1978) require an accurate prediction of entrainment rate. Results for entrainment from free fire plume studies may not be sufficient if disturbances due to room openings are significant. As the present study shows, these "wind" effects could increase the rate of entrainment over free plumes by as great as two to three times. Although the dimensionless correlations and non-reacting plume theory offer ways to explain and generalize the results, they are too empirical and incomplete to be used for general predictions. Variables, such as the distance of the fire from the opening, the elevation of the fire, and the extent to which it may be baffled by other objects all can alter the results of the present study. While it may not be practical or possible to account for these effects in room fire analyses, the present results serve to illustrate the departure from ideal concepts encountered in even a simple room fire configuration,

NOMENCLATURE

A	area
b	plume radius
b_0	plume initial radius
B	dimensionless radius, b/b_0
c_p	specific heat
g	gravitational acceleration
H_0	height of opening
$\dot{m}_a$	rate of air flow
$\dot{m}_e$	rate of mass entrained by fire
$\dot{m}_j$	rate of hot layer fluid mixed into air stream
$\dot{m}_{pt}$	rate of mass entrained by a point source plume
N	height of hot layer in the opening
Q	rate of energy release
s	position along plume trajectory
T	temperature
u	velocity along plume trajectory
u_*	characteristic plume velocity
U	dimensionless plume velocity, u/u_*
v	horizontal wind velocity
V	dimensionless wind speed, v/u_*
W_0	width of opening
z	vertical coordinate
z_i	position of hot layer in room, and the entrainment height

Greek Symbols

α	1st entrainment constant
β	2nd entrainment constant (due to shear velocity)
ΔH	heat of reaction
ξ	dimensionless trajectory position, s/b_0
ϕ	dimensionless temperature, $(T-T_\infty)/T_\infty$
ρ	density

Subscripts

a	air
f	fuel
l	room lower layer
u	room upper layer
∞	ambient

REFERENCES

Brzustowski, T. A. (1978). Hydrocarbon turbulent diffusion flame in subsource cross flow. In *Turbulent Combustion*, L. A. Kennedy (Ed.), *Progress in Astronautics and Aeronautics*, Vol. 58, AIAA, pp. 407–430.

Emmons, H. W. (1978) The prediction of fires in buildings. *17th Symposium (International) on Combustion*, The Combustion Institute, pp. 1101–1111.

Escudier, M. P. (1972). Aerodynamics of a burning turbulent gas jet in a cross flow. *Combustion Science and Technology*, **4**, 293–301.

Hoult, D. P., Fay, J. A., and Forney, L. J. (1969). A theory of plume rise compared with field observations. *T. Air Pullut. Control Assoc.* **19**, 391.

McCaffrey, B. J. (1979). Purely buoyant diffusion flames: Some experimental results. National Bureau of Standards, NBSIR 79-1910.

McCaffrey, B. J., and Rockett, J. A. (1977). Static pressure measurements of enclosure fires. *Jour. of Res.*, National Bureau of Standards, **82**, (2).

Pipkin, O. A., and Sliepcevich, C. M. (1964). Effect of wind on buoyant diffusion flames. *I. and E.C. Fundamentals*, **3** (2), 147–154.

Raj, P. P. K., Moussa, A. N., and Aravamudau, K. (1979). Experiments involving pool and vapor fires from spills of liquidified natural gas on water. Prepared for U.S. Dept. of Transportation, U.S. Coast Guard, Rept. No. CG-D-55-79, No. CG-D-55-79.

Steckler, K. (1980). Fire induced flows through room openings—flow coefficients. Armstrong Cork Co. Report or presentation at the 1980 Fall Technical Meeting, Eastern Section: Combustion Institute, Princeton, New Jersey.

Steward, F. R. (1970). Prediction of the height of turbulent diffusion buoyant flames. *Combustion Science and Technology*, (**2**), 203–212.

Thomas, P. H. (1964). The effect of wind on plumes from a line heat source. F.R. Note No. 572, Fire Research Station, Borehamwood, England.

Thomas, P. H., Pickart, R. W., and Wright, H. G. H. (1963). On the size and orientation of buoyant diffusion flames and the effect of wind. F.R. Note No. 516, Fire Res. Sta., Borehamwood, England.

Welker, J. R., Pipkin, O. A., and Sliepcevich, C. M. (1965). The effect of wind on flames. *Fire Technology*, **1** (2).

Zukoski, E. E., Kubota, T., and Cetegen, G. (1980). Entrainment in fire plumes. Cal. Inst. Tech. Rept., DOC Grant G-9014.